Human Molecular Genetics, 2014, Vol. 23, No. 25 **6722–6731**
doi:10.1093/hmg/ddu390
Advance Access published on July 28, 2014

Excess SMAD signaling contributes to heart and muscle dysfunction in muscular dystrophy

Jeffery A. Goldstein[1], Sasha Bogdanovich[1], Anastasia Beiriger[2], Lisa M. Wren[1], Ann E. Rossi[1], Quan Q. Gao[2], Brandon B. Gardner[1], Judy U. Earley[1], Jeffery D. Molkentin[4] and Elizabeth M. McNally[1,3,*]

[1]Department of Medicine, [2]Committee on Development, Regeneration, and Stem Cell Biology, [3]Department of Human Genetics, The University of Chicago, Chicago, IL, USA and [4]Cincinnati Children's Hospital Medical Center, Department of Pediatrics, and Howard Hughes Medical Institutes, University of Cincinnati, Cincinnati, 240 Albert Sabin Way, Cincinnati, OH 45229, USA

Received June 24, 2014; Revised and Accepted July 23, 2014

Disruption of the dystrophin complex causes muscle injury, dysfunction, cell death and fibrosis. Excess transforming growth factor (TGF) β signaling has been described in human muscular dystrophy and animal models, where it is thought to relate to the progressive fibrosis that characterizes dystrophic muscle. We now found that canonical TGFβ signaling acutely increases when dystrophic muscle is stimulated to contract. Muscle lacking the dystrophin-associated protein γ-sarcoglycan (*Sgcg* null) was subjected to a lengthening protocol to produce maximal muscle injury, which produced rapid accumulation of nuclear phosphorylated SMAD2/3. To test whether reducing SMAD signaling improves muscular dystrophy in mice, we introduced a heterozygous mutation of SMAD4 (S4) into *Sgcg* mice to reduce but not ablate SMAD4. *Sgcg/S4* mice had improved body mass compared with *Sgcg* mice, which normally show a wasting phenotype similar to human muscular dystrophy patients. *Sgcg/S4* mice had improved cardiac function as well as improved twitch and tetanic force in skeletal muscle. Functional enhancement in *Sgcg/S4* muscle occurred without a reduction in fibrosis, suggesting that intracellular SMAD4 targets may be important. An assessment of genes differentially expressed in *Sgcg* muscle focused on those encoding calcium-handling proteins and responsive to TGFβ since this pathway is a target for mediating improvement in muscular dystrophy. These data demonstrate that excessive TGFβ signaling alters cardiac and muscle performance through the intracellular SMAD pathway.

INTRODUCTION

Transforming growth factor-β (TGFβ) is a cytokine with broad effects in tissue growth and repair. Modulation of TGFβ is known to exert its effects through fibrosis, and increased TGFβ signaling has been demonstrated in diseases characterized by excessive fibrosis such as Marfan syndrome, renal fibrosis and chronic obstructive pulmonary disease (1–3). Muscular dystrophy is a progressive degenerative disorder with fibrotic replacement of muscle and increased TGFβ signaling. TGFβ1 levels are increased in Duchenne muscular dystrophy (DMD), an X-linked recessive disorder that arises from mutations in the *DMD* gene (4,5). DMD is the most common X-linked form of muscular dystrophy and shares similar features with other forms of muscular dystrophy, particularly the autosomal recessive muscular dystrophies arising from loss-of-function mutations in the dystrophin-associated proteins the sarcoglycans. Elevated TGFβ has been described in many forms of muscular dystrophy (6).

The *DMD* gene encodes dystrophin, a protein that participates with dystroglycan, sarcoglycans and laminin to form a mechanical link between actin within the myocytes and the extracellular matrix without (7). Recessive mutations in *Sgcg* encoding the dystrophin-associated protein, γ-sarcoglycan, result in muscular dystrophy in humans that is clinically indistinguishable from DMD (8). An engineered mutation in mouse *Sgcg* recapitulates the phenotype of human limb girdle muscular dystrophy (9) including muscle weakness and cardiomyopathy. Disruption of the

*To whom correspondence should be addressed at: The University of Chicago, 5841 S. Maryland MC6088, Chicago, IL 60637, USA. Tel: +1 7737022672; Fax: +1 7737022681; Email: emcnally@uchicago.edu

dystrophin complex is associated with abnormal muscle membrane permeability, muscle cell death and fibrosis. It was previously shown that TGFβ neutralizing antibodies afford some level of protection, albeit incomplete, in the mouse model of DMD, the mdx mouse (10,11). Treatment of the *mdx* mouse model of DMD using an anti-TGFβ antibody improves regeneration, reduces fibrosis and improves pulmonary function (10,11). The anti-TGFβ antibody used in these studies, 1D11, targets multiple TGFβ forms with high affinity (12).

TGFβ binds to a heteromeric complex of TGFβ receptor I and II on the plasma membrane (13). These receptors phosphorylate an intracellular receptor SMAD, either SMAD2 or SMAD3, which then complexes with the co-SMAD, SMAD4, before entering the nucleus and acting to change gene transcription. While there are over 30 TGFβ superfamily members, there are only five receptor SMADs (1, 2, 3, 5 and 8), and SMAD4 is the only co-SMAD. SMADs can also be acted upon by a variety of other signaling, including extracellular-regulated kinase (ERK), Jun N-terminal kinase and cyclin-dependent kinase signaling (13). Notably, TGFβ itself can act in noncanonical pathways through TGFβ-activated kinase-1 that in turn cross-talks with multiple signaling pathways (14). The mechanisms by which TGFβ blockade exerts its effect on multiple aspects of muscular dystrophy have not been delineated.

To test the role of intracellular TGFβ signaling as a mediator of muscle damage, we now used a genetic method to reduce TGFβ signaling in a murine model of muscular dystrophy. A heterozygous SMAD4 (S4) allele was bred into mice lacking γ-sarcoglycan, *Sgcg*, a model for muscular dystrophy. Reduction of the co-SMAD, SMAD4, takes advantage of the broad effect of SMAD4 in the canonical TGFβ intracellular signaling cascade. *Sgcg* mice were used in these studies because they display a more profound cardiac phenotype than the commonly used *mdx* mouse (9). We found that genetic reduction of SMAD4 in *Sgcg* mice (referred to as *Sgcg/S4*) resulted in improved cardiac function and muscle function. Improved function was not accompanied by a reduction in fibrosis, as may be expected for the TGFβ signaling reduction. Instead, a reduction in membrane damage was noted. We hypothesized that SMAD4 may act by altering gene expression in muscle and identified the gene encoding the calcium-handling protein sorcin as a TGFβ responsive gene that is positioned to mediate muscle and heart dysfunction.

RESULTS

Muscle injury induces SMAD signaling

Muscle with dystrophin or sarcoglycan gene mutations has a plasma membrane that is highly susceptible to disruption and injury. We examined whether eccentric contraction was sufficient to induce SMAD signaling in muscle from mice lacking γ-sarcoglycan (*Sgcg* mice) (9). In this study *Sgcg* mice were from a mixed genetic background that was >85% DBA2J; importantly, all mice carried the homozygous deletion allele of *Ltbp4*, which confers a more severe phenotype (15). During eccentric contraction, muscle is contracted and lengthened simultaneously to induce strain on the muscle membrane (16). Contracted *Sgcg* muscle showed extensive nuclear pSMAD3, and uncontracted control myofibers showed many fewer pSMAD-positive nuclei (Fig. 1). An increase in total fibers with pSMAD-positive nuclei was induced by contraction as well as an increase in the total number of pSMAD-positive nuclei per section was seen. The increase in pSMAD-positive nuclei was most evident in centrally positioned nuclei.

In muscular dystrophy, the increase in pSMAD is likely a consequence of the repetitive and ongoing muscle damage that arises from the weakened sarcolemma. Increased TGFβ is seen in response to injury in many tissues. To compare the amount of TGFβ signaling induced in muscular dystrophy versus a more general injury process, wild-type mice with an SMAD reporter allele were studied (17). The SMAD reporter allele drives luciferase activity in response to increased intranuclear pSMAD (17). Cardiotoxin injection produced a measurable increase in luciferase (Supplementary Material, Fig. S1). However, *Sgcg* mice with the luciferase reporter allele did not show an increase in luciferase activity. This is likely due to the insensitivity of the luciferase reporter to detect the lower levels of increased SMAD activity produced in muscular dystrophy. Cardiotoxin injury produces a greater acute injury than muscular dystrophy, but muscular dystrophy is associated with a persistent, lower level injury.

Genetic reduction in SMAD signaling prevents wasting in muscular dystrophy

To study the role of SMAD signaling in muscular dystrophy, mice with a deletion of exon 2 in *SMAD4* (18) were bred to *Sgcg* mice. *SMAD4* encodes the co-SMAD, which is required for all canonical SMAD signaling. In the homozygous state, this SMAD4 deletion is lethal, but heterozygotes are viable

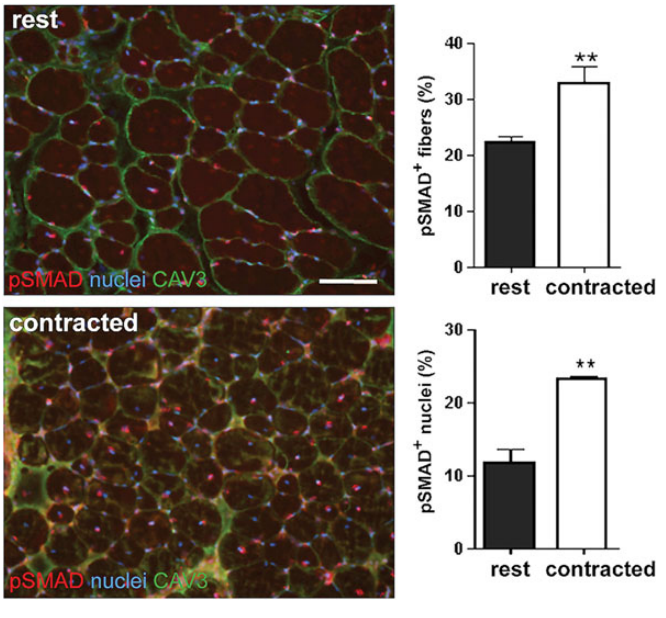

Figure 1. SMAD signaling is increased by contraction in dystrophic muscle. Muscles from mice lacking γ-sarcoglycan, *Sgcg* a model for muscular dystrophy, were studied *ex vivo*. Muscle was subject to acute lengthening contraction, a process that is known to induce damage to muscle with dystrophin and sarcoglycan mutations. Phosphorylated SMAD (pSMAD, red) was increased in *Sgcg* muscle after contraction compared with control *Sgcg* muscle (rest) (scale bar: 30 μm, and $^{**}P < 0.05$).

and fertile. In heterozygous skeletal and cardiac muscle, immunoblotting showed a decrease in SMAD4 protein and the presence of a smaller form (Supplementary Material, Fig. S2). This smaller form is predicted to derive from an amino-terminal truncation and use of an internal ATG residue; amino-terminal truncation of SMAD4 does not disrupt SMAD heterodimers (19). *Sgcg/S4* refers to *Sgcg* null mice with the heterozygous SMAD4 allele. Mice were examined at 12 and 24 weeks and compared with littermate *Sgcg* mice. Failure to gain mass is a feature of *Sgcg* mice (20). We found that *Sgcg*/S4 males weigh more than *Sgcg* males, and that overall, *Sgcg*/S4 mice weigh more when the mass is normalized for tibia length (Fig. 2).

Reduction in SMAD signaling leads to larger myofibers

We examined the histopathology in quadriceps femoris muscle from 12-week mice. Sections of muscle from *Sgcg* and *Sgcg/S4* mice appeared grossly similar in that centrally nucleated myofibers, fibrosis and immune infiltrates were present in both. Myofibers from *Sgcg/S4* mice had a larger average fiber size, $63.4 \pm 78.1\ \mu m^2$, as opposed to $34.3 \pm 33.2\ \mu m^2$ for *Sgcg* mice ($n = 200$ fibers, $P < 0.001$; Fig. 3B). This was reflected in an increased number of the largest fibers, those $>100\ \mu m^2$, which were 8 of 200 *Sgcg* fibers and 42 of 200 *Sgcg/S4* fibers.

Improved *ex vivo* muscle function by genetically reducing SMAD4

Progressive loss of skeletal muscle function is another hallmark feature of muscular dystrophy. Weakness is manifest in muscle in the form of lower specific force, the amount of force generated per muscle area. We examined muscle mechanics in the extensor digitorum longus (EDL) muscle of 24-week-old mice and tested *ex vivo* contraction properties. We found that compared with *Sgcg* mice, *Sgcg/S4* mice generated greater twitch force ($11.10 \pm 0.44\ mN/mm^2$ versus $6.62 \pm 0.40\ mN/mm^2$, $P < 0.0001$) and greater (tetanic force, $54.42 \pm 2.50\ mN/mm^2$ versus $31.84 \pm 1.79\ mN/mm^2$) ($P < 0.0001$). This improvement reflects increased skeletal muscle functionality (Fig. 4).

Improved heart function in *Sgcg/S4* mice

Heart failure is a cardinal feature of many forms of muscular dystrophy, including DMD and limb girdle muscular dystrophy from *Sgcg* mutations. We measured heart function in using echocardiography and found improved function in *Sgcg/S4* mice compared with *Sgcg* mice. At 12 weeks of age, *Sgcg/S4* mice had a reduced ventricular dilation (2.71 ± 0.34 mm versus 3.06 ± 0.37 mm, $n = 6$ and 3 mice, $P < 0.05$), and an improved fractional shortening ($30.6 \pm 6.6\%$ versus $22.6 \pm 7.4\%$, $P < 0.01$). At 24 weeks, this improvement in heart function was more apparent. Compared with *Sgcg* mice, *Sgcg/S4* mice had improved fractional shortening (23.2 ± 1.4 versus 31.6 ± 1.7), ejection fraction (45.1 ± 2.8 versus 59.7 ± 2.4) and reduced ventricular dilation (3.07 ± 0.10 versus 2.70 ± 0.08) (Fig. 5). This data support that reducing SMAD signaling reduces the progressive cardiomyopathy from loss of *Sgcg*.

Persistent fibrosis in *Sgcg/S4* mice

We assessed fibrosis by chemically measuring hydroxyproline (HOP), a modified amino acid found in collagen, the major component of scar tissue. In comparison to *Sgcg* mice, *Sgcg/S4* mice did not show a significant reduction in this quantitative measure of fibrosis in quadriceps or the right and left ventricles (Fig. 6). Other muscle groups, such as the abdominal muscles and diaphragm muscle, also did not show a reduction in HOP content (data not shown). This suggests that functional improvement seen in the heart and skeletal muscle is not simply due to less replacement of muscle by scar tissue and supports that additional, potentially cell-intrinsic mechanisms may be responsible.

Evan's blue dye is a small molecule that binds to circulating albumin and enters muscle cells as a result of membrane injury of cellular breakdown (21). We interrogated this measure of cellular injury at 24 weeks of age and found that the quadriceps muscle showed evidence of reduced dye uptake (0.73 ± 0.09 versus 1.07 ± 0.13, $P < 0.01$, $n = 6$ and 3 mice). This reduction in Evans blue dye permeability was not seen for other muscle groups including the gastrocnemius-soleus, triceps, abdominals and gluteus/hamstrings (data not shown). However, the large

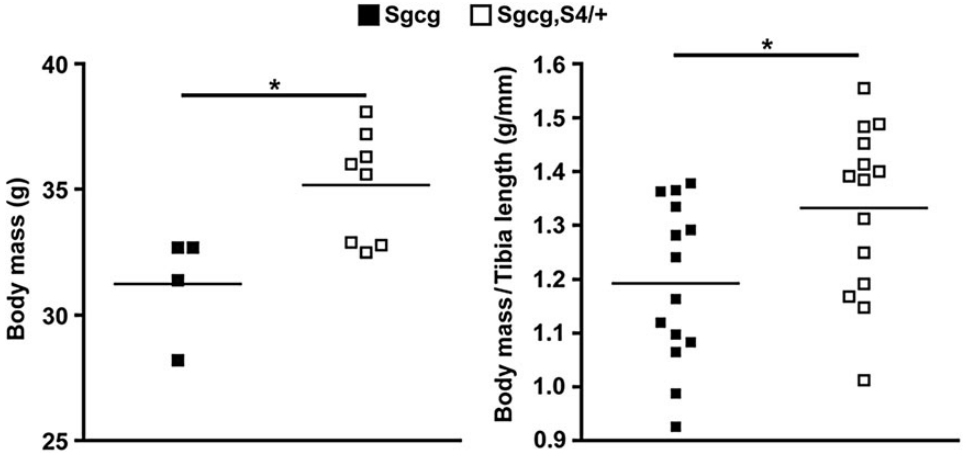

Figure 2. Increased body mass in *Sgcg,S4/+* mice. To study the role of SMAD signaling in muscular dystrophy, mice with a targeted mutation in SMAD4 (18) were bred with *Sgcg* mice. At 12 weeks of age, *Sgcg* mice have weight loss and wasting (20). In contrast, *Sgcg/S4* mice maintained mass better ($P < 0.05$). When normalizing mass for tibia length to control for differences in body size, *Sgcg/S4* mice were heavier ($P < 0.05$).

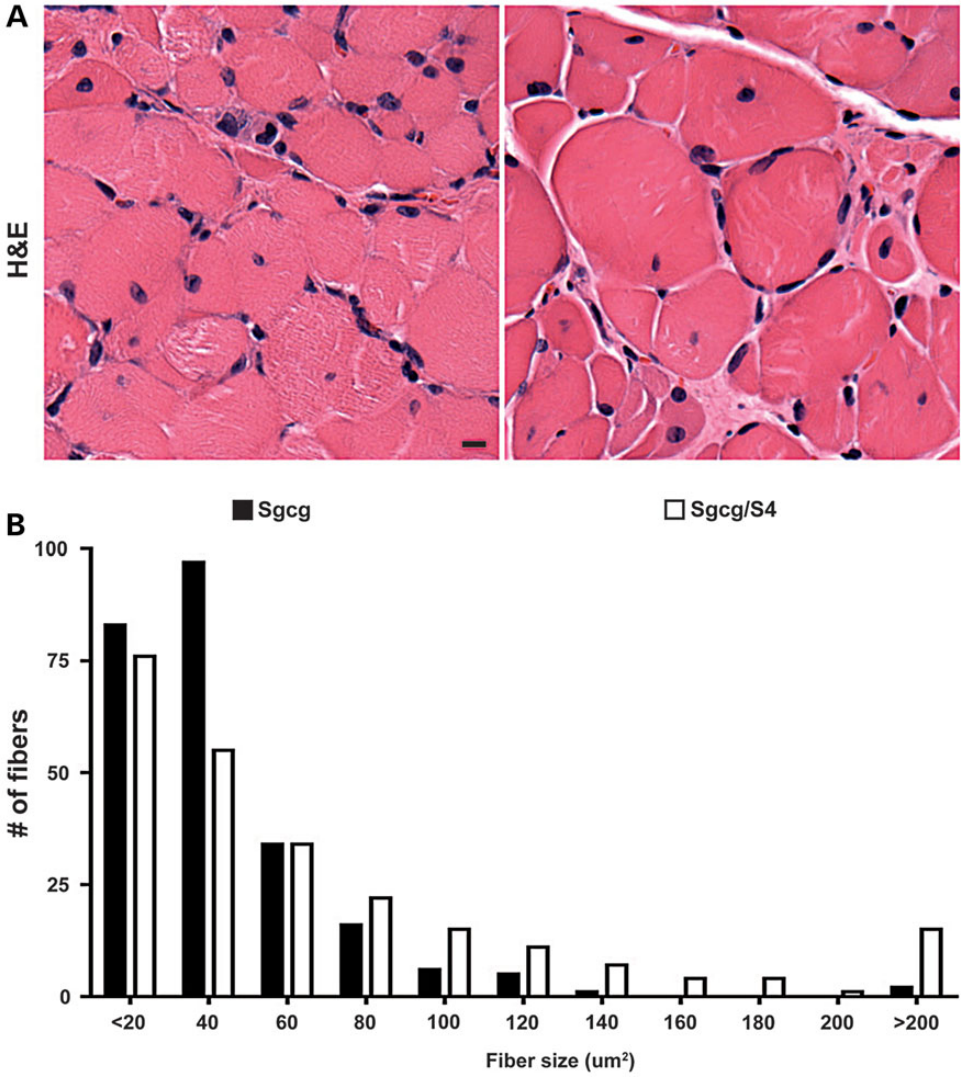

Figure 3. *Sgcg/S4* mice have larger myofibers than Sgcg mice. (**A**) H&E stained quadriceps muscle from 12 week animals. (**B**) Fiber size distribution in quadriceps muscle. Sgcg/S4 mice have larger average myofiber diameter and this is reflected in this distribution where larger fibers are seen in Sgcg/S4 muscle ($P < 0.001$). Scale bar: 10 μm.

size and exercise demands on the quadriceps muscles may make this a better muscle group to analyze. The decrease in membrane leak suggested that intracellular muscle pathways may be altered by SMAD signaling.

Alteration in calcium-handling genes in *Sgcg* muscle

We queried gene expression data to identify genes important for calcium regulation that were differentially expressed in *Sgcg* heart and muscle. We focused on calcium-handling proteins in the sarcoplasmic reticulum (SR) since it was previously shown that calcium overload is sufficient to produce a muscular dystrophy phenotype and that SERCA overexpression can ameliorate features of muscular dystrophy (22,23). We hypothesized that some of these transcriptional changes were a direct result of stimulation by TGFβ and focused our attention on genes that have predicted SMAD-binding elements upstream. This analysis, although not exhaustive, identified several candidate genes that were tested by assessing whether TGFβ exposure increased their expression. Differentiated C2C12 myotubes were treated with TGFβ and quantitative RT-PCR was conducted. As a positive control, TGFβ produced the expected upregulation of SMAD7 (3.42 ± 1.53-fold above unstimulated, $P < 0.05$; Fig. 7). Although several calcium-handling genes were tested, only sorcin mRNA increased in response to TGFβ. Sorcin mRNA was upregulated by TGFβ exposure (1.86 ± 0.06-fold, $P < 0.01$; Fig. 7). Sorcin interacts with both the ryanodine receptor and the sodium calcium exchanger (24–26), and therefore is positioned to alter intracellular calcium and muscle function.

Quantitative RT-PCR to detect sorcin mRNA demonstrated an increase in sorcin in *Sgcg* muscle with a reduction in *Sgcg/S4* muscle (Fig. 8). Immunoblotting with an anti-sorcin antibody showed an increase in sorcin in *Sgcg* muscle, which was also confirmed using immunofluorescence microscopy (Fig. 8C). The increase in sorcin expression was seen diffusely throughout the myoplasm as well as at the membrane. Sarcolipin mRNA, which was the gene most highly expressed in *Sgcg* muscle

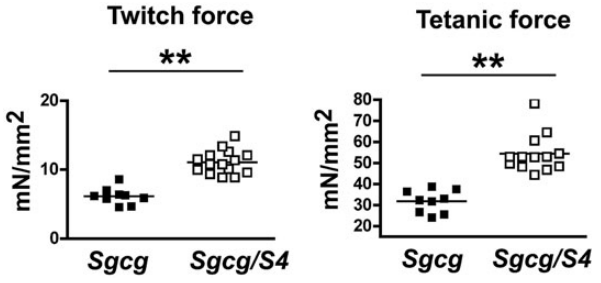

Figure 4. Increased muscle strength in *Sgcg/S4* mice. Twitch and tetanic force were measured *ex vivo* on the excised extensor EDL muscle from 24-week animals. (**A**) Twitch and (**B**) tetanic force is improved in *Sgcg/S4* muscle compared with *Sgcg* ($P < 0.005$ for both comparisons). These data are consistent with suppression of the weakness that is a hallmark of muscular dystrophy.

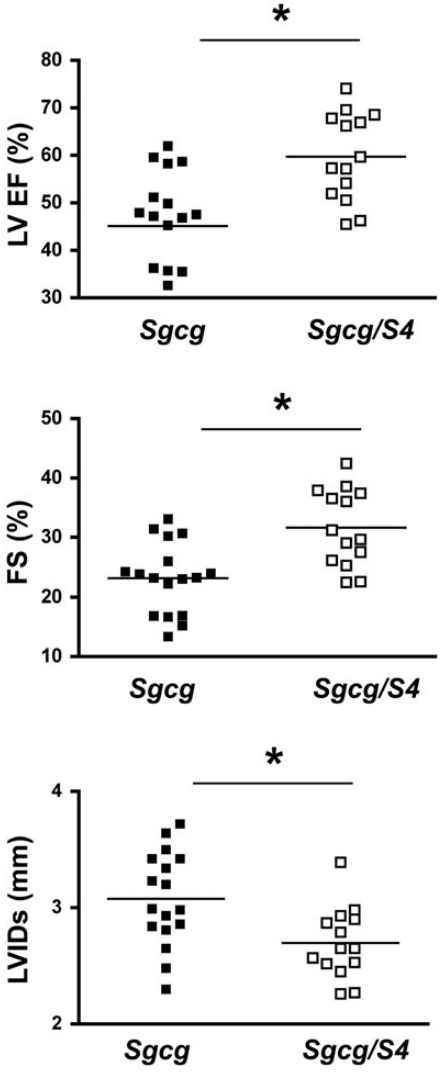

Figure 5. Improved heart function in *Sgcg/S4* mice. *Sgcg/S4* hearts had an improved left ventricular ejection fraction (LVEF) and fractional shortening (FS) compared with *Sgcg* mice ($P < 0.005$). Left ventricular dilation was also reduced in Sgcg/S4 mice compared with Sgcg mice with a decreased in the left ventricular internal diameter in systole (LVIDs) ($P < 0.005$).

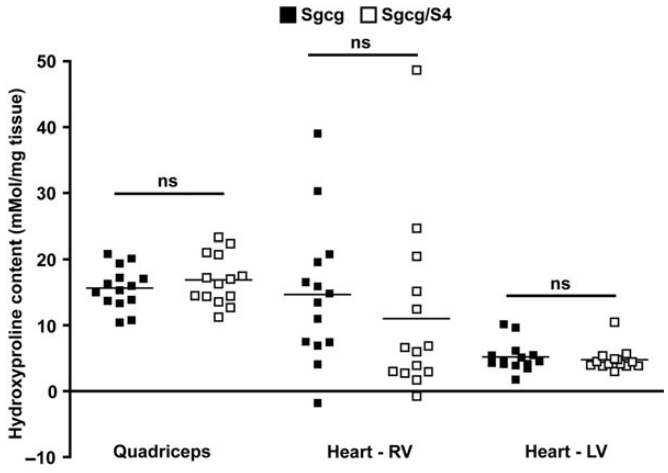

Figure 6. Unchanged fibrosis in *Sgcg/S4.* Muscle fibrosis is a hallmark of muscular dystrophy. Fibrosis was measured by determining hydroxyproline content, a modified amino acid found only in collagen, the major constituent in fibrous tissue. There was no difference between *Sgcg/S4* and *Sgcg* mice in any tissue at either 12 or 24 weeks.

compared with WT (Fig. 7), was also found to be elevated in *Sgcg* muscle and decreased by the presence of the S4 allele. These data suggest that nuclear SMAD may act on a complex of genes in the calcium-handling pathway to improve muscle function in muscular dystrophy.

DISCUSSION

Reducing SMAD4 improves heart and muscle function

Canonical TGFβ signaling was reduced using a genetic approach and this was found to suppress key aspects of the muscular dystrophy phenotype, including heart and skeletal muscle dysfunction. Disruption of the dystrophin complex induces TGFβ signaling as a result of muscle injury and increased membrane permeability. Disruption of the muscle membrane in muscular dystrophy induces an injury response similar to but of lesser magnitude than cardiotoxin injury. However, in muscular dystrophy, injury is unrelenting and accumulates outpacing regeneration. The reduction of SMAD signaling induced by the S4 heterozygous allele improved heart and muscle mechanical function. We found a reduction of dye uptake into muscle, supporting the concept that blocking intracellular canonical TGFβ signaling may at least partially act by improving membrane leak and stability and therefore their downstream consequences. Strikingly, reduction in SMAD4 did not reduce fibrosis. Reducing intracellular signaling pathways may directly improve cardiac and muscle strength. These findings are consistent with what was observed when SMAD signaling was reduced in the invertebrate *Drosophila* model, *Sgcd*^{840} (27). Notably, because the fly model lacks fibrosis and cellular infiltrate into muscle, the improvement likely derives from muscle intrinsic effects. Genetic reduction of SMAD signaling in the *Drosophila* model improved heart and muscle function, but did so downstream of muscle disruption, similar to what we observed here.

Myocyte response to TGFβ in muscular dystrophy

In dystrophic muscle, the nonmyogenic cells, such as fibroblasts and invading inflammatory cells, display significant nuclear

Left ventricular sarcoplasmic reticulum cluster				
UNIGENE	GENE NAME	Gene symbol	Fold change	SMAD sites
Mm.12829	calsequestrin 1	Casq1	1.55	18
Mm.34459	junctophilin 2	Jph2	−1.31	6
Mm.34145	phospholamban	Pln	3.36	0
Mm.96211	sorcin	Sri	1.49	1
Mm.212927	transmembrane protein 38A	Tmem38A	−1.14	4
Mm.35134	ATPase, Ca++ transporting, cardiac muscle, fast twitch 1	SERCA	1.05	34
Gastrocnemius sarcoplasmic reticulum cluster				
UNIGENE	GENE NAME	Gene symbol	Fold change	SMAD sites
Mm.15343	calsequestrin 2	Casq2	1.29	4
Mm.227912	inositol 1,4,5-triphosphate receptor 1	Itpr1	−2.83	3
Mm.143761	junctophilin 1	Jph1	−1.63	16
1421453_at	junctophilin 2	Jph2	−1.37	6
1420884_at	sarcolipin	Sln	4.54	10
Mm.96211	sorcin	Sri	1.93	1
Mm.212927	transmembrane protein 38A	Tmem38A	−1.21	4

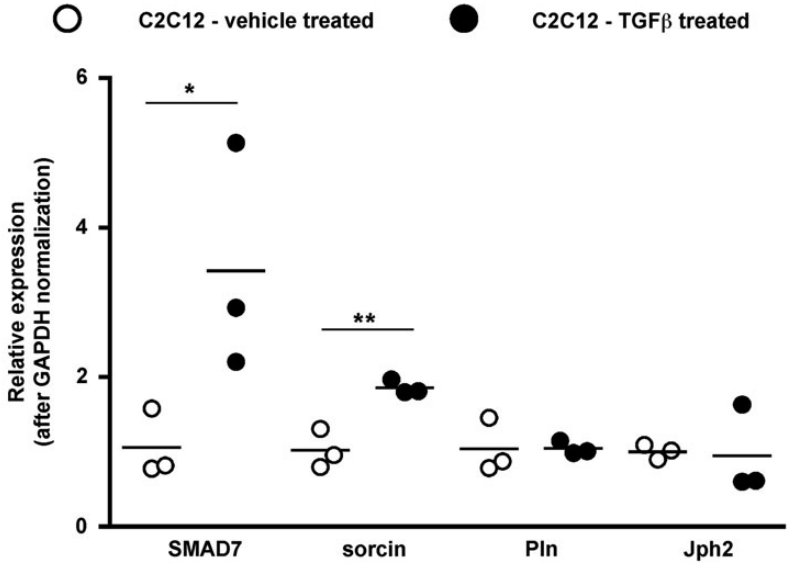

Figure 7. Changes in calcium genes due to TGFβ treatment. A common cluster of genes was identified as misexpressed in *Sgcg* compared with strain-matched wild-type heart and muscle. We focused on genes related to calcium handling in the SR since SERCA overexpression is known to ameliorate features of muscular dystrophy (23). To demonstrate whether these genes are SMAD4 targets, we exposed differentiated C2C12 myotubes to recombinant TGFβ. The known SMAD4 target, SMAD7, responded as expected. Of the three tested genes, only sorcin was upregulated by TGFβ.

pSMAD. However, myofiber nuclei also have elevated pSMAD in muscular dystrophy, and this finding is also evident in acute injury. Nuclear accumulation of pSMAD in myofiber nuclei indicates that myofiber-based gene expression may be altered to improve function. This does not exclude the possibility that nonmuscle TGFβ signaling contributes significantly to improved function. Ca^{2+} is a mediator of excitation contraction coupling, and compounds that target calcium handling may lead to improved muscle function in muscular dystrophy (28). Overexpression of SERCA improves the outcome in muscular dystrophy (23), and increasing Ca^{2+} influx into muscle is sufficient to produce muscular dystrophy (22). Because of these observations, we focused our attention on SR-associated proteins that were differentially expressed. We tested several of these genes for their responsiveness to TGFβ. These studies are limited because the cell line in which we performed these studies only expresses a subset of the relevant genes. Nonetheless, we identified sorcin as upregulated in *Sgcg* heart and skeletal muscle and also increased in response to TGFβ exposure. The increase in sorcin expression may derive from both direct SMAD effects and indirect effects. Work from others has shown that sorcin upregulation is a feature of acute heart failure in mice that lack Dicer since it is a target of miR-1 (29). Sorcin interacts with the RyR in a calcium-dependent fashion (24,25) and sorcin overexpression is sufficient to cause contractile deficits and abnormal Ca^{2+} transients (30). While it is likely that other genes contribute to the Ca^{2+} mishandling in dystrophin heart and muscle, at least some of these genes may act through TGFβ signaling pathways.

Receptor based versus intracellular reduction in TGFβ

Secretion of TGFβ is induced by the peptide hormone angiotensin II, and angiotensin receptor blockers have been shown to

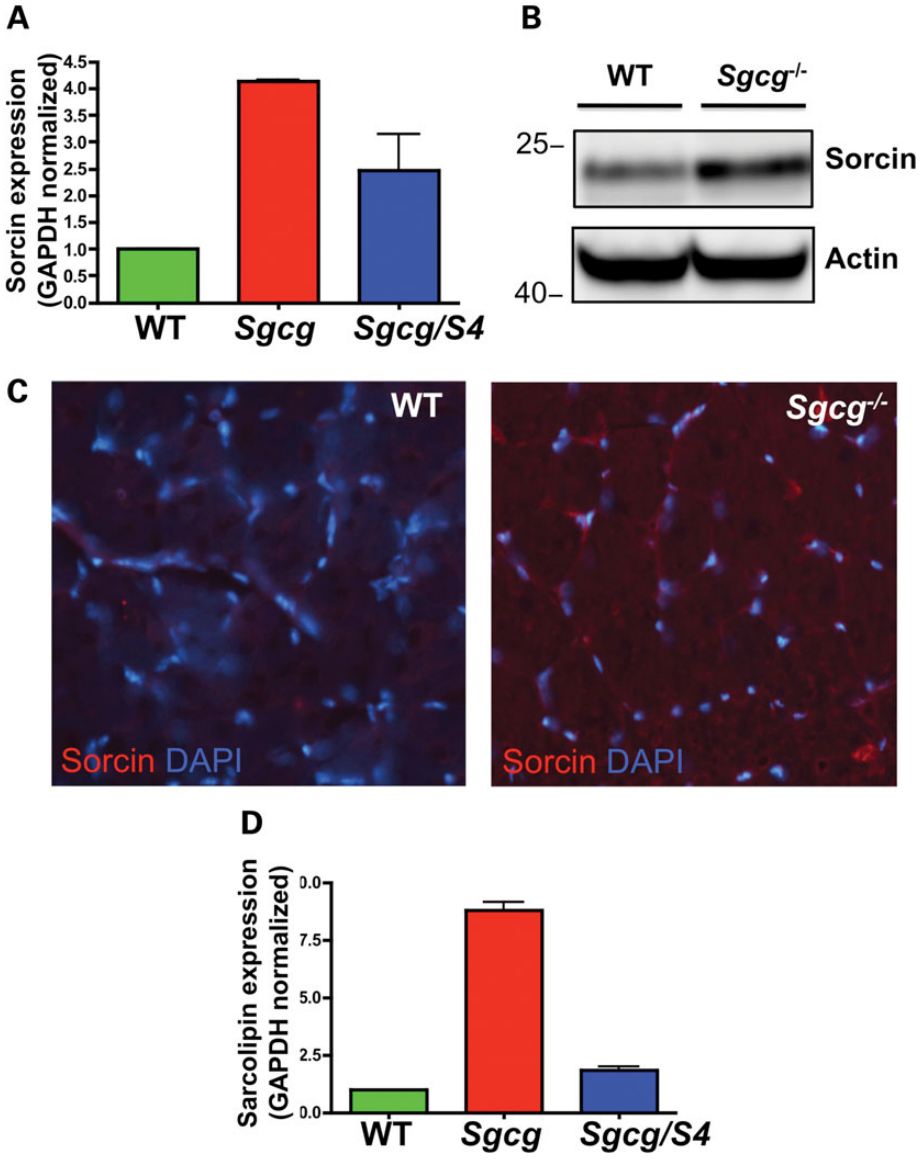

Figure 8. Sorcin is increased in *Sgcg* muscle. (**A**) Quantitative RT-PCR confirmed that sorcin mRNA was upregulated in *Sgcg* muscle and reduced in *Sgcg/S4* muscle. (**B**) Immunoblotting with an anti-sorcin antibody confirmed upregulation in *Sgcg* muscle. (**C**) Immunofluorescence microscopy with an anti-sorcin antibody also showed upregulation in *Sgcg* muscle. (**D**) Sarcolipin mRNA was also increased in *Sgcg* muscle and reduced in *Sgcg/S4* muscle.

improve repair of *mdx* muscle after artificial injury and to increase *ex vivo* and *in vivo* muscle strength (10). Nelson *et al*. found that prolonged injection of 1D11, the anti-TGFβ antibody, improved several aspects of the dystrophy phenotype in mdx mice (11). Genetic reduction of *SMAD4* showed its effect more at 24 versus 12 weeks of age. As the phenotype becomes more profound with age, it is interesting that effect of genetic reduction remained even in the face of more significant deficits.

TGFβ reduction has been studied as a treatment in other forms of heart failure, notably in pressure overload induced by trans-aortic constriction (31). As with muscular dystrophy, this model shows interstitial fibrosis. Koitabashi *et al.* noted that anti-TGFβ treatment lowered pSMAD near medium sized blood vessels and reduced fibrosis around those vessels, but it had minimal effects on myocyte pSMAD or fibrosis within the bulk of muscle. The authors suggested that the anti-TGFβ antibody may have limited capacity to penetrate deeply within the tissues, which could be one limitation with adopting this strategy for reducing TGFβ signaling. Reducing intracellular signaling through the SMAD4 allele would not be affected by tissue penetration but also may mediate its effect because it is downstream from multiple TGFβ family members. Together, these data support that therapy aimed at reducing intracellular TGFβ signaling is a viable target to improve heart and muscle performance.

MATERIALS AND METHODS

Animals and harvest

Sgcg mutant mice were generated by deleting exon 2 of *Sgcg* to create a null allele (9). This S*gcg* allele in the DBA2J

background were used (20). Mice were selected to be homozygous for the *Ltbp4* deletion (15) to avoid the modifier effect of the insertion/deletion in the *Ltbp4*. SBE-luc mice, formally B6.Cg-Tg(SBE/TK-luc)7Twc/J (17) (Jackson Laboratory strain 005999), were used to detect SMAD activity. The $SMAD4^{f}$ allele used in these studies flanked exon 2 of *SMAD4* with loxP sites (18). These mice were bred with Mox2-cre mice, which express Cre recombinase in the germline (32) (Jackson Laboratory strain 003755). The resulting $SMAD^{N/+}$ mice were outcrossed to remove the Mox2-cre transgene, bred with *Sgcg* mice, and then bred to additional *Sgcg* null mice to generate appropriate genotypes (*Sgcg* and *Sgcg/S4* indicating SMAD4 heterozygous mice).

Mice were analyzed at 8, 12 or 24 weeks as indicated and compared with littermate controls. Mice were housed under the auspices of the Animal Care and Use Committee and Animal Resources Center at the University of Chicago. The order of harvest was chosen to minimize interference of one assay with the next. Two days prior to harvest, mice were weighed and injected Evan's blue. On the subsequent day, grip strength measurement and echocardiography were performed. On the day of harvest, serum was collected immediately prior to sacrifice, and collection of the muscles for *ex vivo* measurement occurred immediately after. Tissues were weighed at the time of collection and the tibia length was measured using a millimeter ruler after being stripped of muscle.

Antibodies

Goat anti-phosphorylated SMAD2/3 (pSMAD2/3), # sc11769 was from Santa Cruz Biotechnology or from Abcam to pSMAD3 (ab51451). The sorcin antibody was a generous gift from Hector Valdivia (33). Rabbit anti-laminin # L9393 was from Sigma. Goat anti-rabbit IgG # 111-035-003 was from Jackson Immunoresearch. Donkey anti-rabbit IgG Alexa 488 conjugate (DaR-488), # A-21208 and Donkey anti-goat IgG Alexa 594 conjugate (DaG-594), # A-11058 were from Invitrogen. Anti-TGFβ antibody (1D11) (12) and control 13C4 were obtained from Genzyme Corporation (Framingham, MA, USA).

Ex vivo muscle contraction

Intact extensor EDL muscles were excised in regular rodent Ringer's solution (in mM: 146 NaCl, 5 KCl, 2 $CaCl_2$, 1 $MgCl_2$ and 10 HEPES, pH 7.4) essentially according to the TREAT-NMD standard operating procedure (34). Muscles were suspended in a vertical tissue bath containing oxygenated Kreb's solution (in mM: 121 NaCl, 5 KCl, 1.8 $CaCl_2$, 0.5 $MgCl_2$, 0.1 EDTA, 0.4 NaH_2PO_4, 24 $NaHCO_3$ and 5 glucose, pH 7.4, with continuous bubbling 95% O_2/5% CO_2). The distal tendon was attached to a fixed support with 6-0 silk suture, while the proximal tendon was tied to the lever arm of a force transducer (Aurora Scientific, 300C-LR). The isolated muscles were stimulated with 0.5 ms pulses at 1 A via two parallel platinum electrodes flaking the muscle. The length of each EDL was adjusted to that which produced the maximal twitch force (L0), which was measured using fine calipers. Maximal twitch and tetanic force were elicited with a series of 3 trains, 3 min apart. The data were combined from three separate animals of each genotype. Males were used for these studies since there were baseline differences between sexes in Sgcg mice. Subsequently, each EDL was subjected to an eccentric contraction protocol, which consisted of five 700 ms, 80 Hz tetani with a lengthening by 10% of L0 during the last 200 ms of each tetanus. At the conclusion of each experiment, each muscle was blotted and immediately weighed. All data were analyzed offline following data import into Clampfit software (Molecular Devices, Clampfit v10.2.0.14). All force measurements (P_0) were normalized to cross-sectional area and expressed as specific force (sP_0; mN/mm^2), which was calculated according to the following equation:

$$sP_0 = \frac{P_0}{\{\text{muscle mass}/[(L_0 \times 0.44) \times 1.06\ \text{g/m}^2]\}},$$

where 0.44 is the muscle length to fiber length ratio for EDL, and 1.06 is the density of muscle (34).

Immunofluorescence microscopy

After eccentric contraction, EDL muscles were maintained in oxygenated nutrient back for 1 h to allow for signaling, then snap frozen in liquid nitrogen-chilled isopentane. Samples were processed similarly to a previously published method (35). Ten micrometers sections were cut and sections were fixed for 10 min in ethanol on ice. Sections were blocked for 1 h at 4°C in 10% fetal bovine serum (FBS), 0.03% Triton X-100 in phosphate-buffered saline (PBS). Samples were incubated overnight at 4°C in 1% FBS, 0.03% Triton X-100, PBS with 1 : 100 dilution of anti-pSMAD2/3 and 1:200 anti-laminin. Samples were washed three times with 0.03% Triton X-100, PBS on ice for 15 min. DaG-594 and DaR-488 were applied for 3 h at 4°C in 1% FBS 0.03% Triton X-100, PBS. Slides were again washed, and mounted using Vectashield with DAPI (Vector Laboratories). Images were collected at ×40 original magnification using an Axiophot microscope with iVision software and manipulated within NIH guidelines using Adobe Photoshop CS4 and ImageJ.

Histology

A cross-sectional disc of muscle was harvested from the mid-belly of the quadriceps muscle. The disc was fixed in formalin, dehydrated, paraffin embedded, sectioned at 6 μm thickness and stained using hematoxylin and eosin (H&E). For analysis of central nuclei, five random fields each were collected from five mice of each genotype (total 25 sections). The number of fibers and number of fibers with at least one non-peripheral nucleus were counted and the ratio calculated. For fiber size, fibers were outlined using Adobe Photoshop CS4 or the GNU Image Manipulation Program 2.0.2. Fiber size was determined using ImageJ. Two hundred fibers were counted for each genotype.

Echocardiography

Mice were depilated, anesthetized with isoflurane and placed on a 37°C warming pad. Anesthesia was titrated to produce a heart rate of 350–450 beats/min. Left ventricular dimensions were quantified by transthoracic echocardiography using a

VisualSonics Vevo 770 ultrasound (Toronto, ON, Canada). Two-dimensional parasternal short-axis M-mode images were acquired and analyzed offline. Fractional shortening was calculated using (diastolic diameter − systolic diameter)/diastolic diameter × 100%. All measurements were done by the same operator, who was blinded to treatment and genotype at the time of measurements.

Evan's blue dye uptake assay and hydroxyproline assay

This assay was performed essentially according to (20). Mice were injected intraperitoneally with 5 μl/g of a 10 mg/ml solution of EBD in PBS. Tissues were collected at harvest and submerged in 1 ml deionized formamide, then incubated for 2.5–4 h until all dye had visibly been extracted. The supernatant was decanted and absorbance at 620 nm was measured. Absorbance values were normalized for the weight of the tissue, and the absorbance/weight of the kidney, a measure of circulating dye levels. Tissue HOP content was determined as previously reported (20).

Response of muscle cells to TGFβ

C2C12 cells were obtained from ATCC and studied at passages 16–19. Cells were grown at 37°C in 5% CO_2. Cells were expanded in growth medium, 10%FBS, 1% penicillin/streptomycin, DMEM. Confluent cells were differentiated in 2% horse serum, 1% penicillin/streptomycin, DMEM for 4 days, with the medium changed at Day 2. For TGFβ stimulation, differentiation medium was supplemented with 5μg/ml TGFβ or vehicle (4 mM HCl, 0.1% bovine serum albumin) for 3 h. Recombinant human TGFβ1, # 240-B was from R&D Systems (Minneapolis, MN, USA). Three replicate cultures were studied for each treatment. RNA was extracted with the Trizol RNA extraction kit #12183–555 (Invitrogen). Genomic DNA was removed with the RNAse free DNAse set #79254 (Qiagen). RNA was reverse transcribed with qScript cDNA Supermix # 95048-25 (Quanta Biosciences, Gaithersberg, MD, USA) and qPCR was done using SsoAdvanced SYBR® Green Supermix #172–5260 (Bio-Rad). SMAD7, Sri, Pln and Jph2 primers were in the form of PrimeTime qPCR assays (IDT, Coralville, IA, USA). Relative amounts of mRNA were determined by the following method. The CT was determined automatically for each reaction, and the ΔCT was calculated as the difference between the CT for a gene of interest and GAPDH. The average ΔCT was calculated for the vehicle-treated cells, and a ΔΔCT was calculated as the difference between a given ΔCT and the vehicle average. For each sample, the fold change was calculated as $FC = 2^{-\Delta\Delta CT}$.

Oligonucleotide microarray hybridization and analysis

Mice were sacrificed at postnatal Day 14, 56 or 240 (p14, p56 and p240). Hearts were excised and the right ventricle and atrial tissues above the atrioventricular groove were removed. Bilateral gastrocnemius-soleus muscles were harvested. Tissues were frozen in liquid nitrogen and stored at −80°F. For each time point, tissues from 3 to 8 mice per genotype were pooled and powdered using a liquid nitrogen-cooled mortar and pestle. The pooled tissue was homogenized in Trizol reagent (GibcoBRL, Rockville, MD, USA) and total RNA was extracted. RNA pellets were resuspended in diethylpyrocarbonate-treated water and DNase treated (Turbo DNAfree, Ambion, Austin, TX, USA). RNA quality was assessed by formaldehyde-agarose gel electrophoresis, spectrophotometry (OD 260/280 nm >1.9) and spectral interrogation of ribosomal RNA band integrity (Agilent Bioanalyzer, Agilent Technologies, Palo Alto, CA, USA). RNA concentration was verified by spectrophotometry and an Agilent Bioanalyzer. RNA samples were hybridized to the Affymetrix Mouse Expression Array 430A (MOE430A) at the Functional Genomics Facility at the University of Chicago following the manufacturer's protocol (Affymetrix Incorporated, Santa Clara, CA, USA). For the p240 time point, RNA representing each genotype and tissue was hybridized in triplicate (each RNA sample hybridized to three independent arrays). For the p14 and p56 time points, each genotype was represented by two independent, pooled RNA samples per tissue.

SUPPLEMENTARY MATERIAL

Supplementary Material is available at *HMG* online.

Conflict of Interest statement. None declared.

FUNDING

This work was supported by NIH NS072027, NIH HL61322, NIH HL007381 and NIH GM07281.

REFERENCES

1. Neptune, E.R., Frischmeyer, P.A., Arking, D.E., Myers, L., Bunton, T.E., Gayraud, B., Ramirez, F., Sakai, L.Y. and Dietz, H.C. (2003) Dysregulation of TGF-beta activation contributes to pathogenesis in Marfan syndrome. *Nat. Genet.*, **33**, 407–411.
2. Lan, H.Y. (2011) Diverse roles of TGF-beta/Smads in renal fibrosis and inflammation. *Int. J. Biol. Sci.*, **7**, 1056–1067.
3. Hersh, C.P., Demeo, D.L., Lazarus, R., Celedon, J.C., Raby, B.A., Benditt, J.O., Criner, G., Make, B., Martinez, F.J., Scanlon, P.D. *et al.* (2006) Genetic association analysis of functional impairment in chronic obstructive pulmonary disease. *Am. J. Respir. Crit. Care Med.*, **173**, 977–984.
4. Hoffman, E.P., Brown, R.H. Jr and Kunkel, L.M. (1987) Dystrophin: the protein product of the Duchenne muscular dystrophy locus. *Cell*, **51**, 919–928.
5. Bernasconi, P., Torchiana, E., Confalonieri, P., Brugnoni, R., Barresi, R., Mora, M., Cornelio, F., Morandi, L. and Mantegazza, R. (1995) Expression of transforming growth factor-beta 1 in dystrophic patient muscles correlates with fibrosis. Pathogenetic role of a fibrogenic cytokine. *J. Clin. Invest.*, **96**, 1137–1144.
6. Burks, T.N. and Cohn, R.D. (2011) Role of TGF-beta signaling in inherited and acquired myopathies. *Skelet. Muscle*, **1**, 19.
7. Rybakova, I.N., Patel, J.R. and Ervasti, J.M. (2000) The dystrophin complex forms a mechanically strong link between the sarcolemma and costameric actin. *J. Cell. Biol.*, **150**, 1209–1214.
8. Noguchi, S., McNally, E.M., Ben Othmane, K., Hagiwara, Y., Mizuno, Y., Yoshida, M., Yamamoto, H., Bonnemann, C.G., Gussoni, E., Denton, P.H. *et al.* (1995) Mutations in the dystrophin-associated protein gamma-sarcoglycan in chromosome 13 muscular dystrophy. *Science*, **270**, 819–822.
9. Hack, A.A., Ly, C.T., Jiang, F., Clendenin, C.J., Sigrist, K.S., Wollmann, R.L. and McNally, E.M. (1998) Gamma-sarcoglycan deficiency leads to muscle membrane defects and apoptosis independent of dystrophin. *J. Cell Biol.*, **142**, 1279–1287.
10. Cohn, R.D., van Erp, C., Habashi, J.P., Soleimani, A.A., Klein, E.C., Lisi, M.T., Gamradt, M., ap Rhys, C.M., Holm, T.M., Loeys, B.L. *et al.* (2007) Angiotensin II type 1 receptor blockade attenuates TGF-beta-induced failure

of muscle regeneration in multiple myopathic states. *Nat. Med.*, **13**, 204–210.
11. Nelson, C.A., Hunter, R.B., Quigley, L.A., Girgenrath, S., Weber, W.D., McCullough, J.A., Dinardo, C.J., Keefe, K.A., Ceci, L., Clayton, N.P. *et al.* (2011) Inhibiting TGF-beta activity improves respiratory function in mdx mice. *Am. J. Pathol.*, **178**, 2611–2621.
12. Dasch, J.R., Pace, D.R., Waegell, W., Inenaga, D. and Ellingsworth, L. (1989) Monoclonal antibodies recognizing transforming growth factor-beta. Bioactivity neutralization and transforming growth factor beta 2 affinity purification. *J. Immunol.*, **142**, 1536–1541.
13. Feng, X.H. and Derynck, R. (2005) Specificity and versatility in tgf-beta signaling through Smads. *Annu. Rev. Cell Dev. Biol.*, **21**, 659–693.
14. Delaney, J.R. and Mlodzik, M. (2006) TGF-beta activated kinase-1: new insights into the diverse roles of TAK1 in development and immunity. *Cell Cycle*, **5**, 2852–2855.
15. Heydemann, A., Ceco, E., Lim, J.E., Hadhazy, M., Ryder, P., Moran, J.L., Beier, D.R., Palmer, A.A. and McNally, E.M. (2009) Latent TGF-beta-binding protein 4 modifies muscular dystrophy in mice. *J. Clin. Invest.*, **119**, 3703–3712.
16. Petrof, B.J., Shrager, J.B., Stedman, H.H., Kelly, A.M. and Sweeney, H.L. (1993) Dystrophin protects the sarcolemma from stresses developed during muscle contraction. *Proc. Natl. Acad. Sci. USA*, **90**, 3710–3714.
17. Lin, A.H., Luo, J., Mondshein, L.H., ten Dijke, P., Vivien, D., Contag, C.H. and Wyss-Coray, T. (2005) Global analysis of Smad2/3-dependent TGF-beta signaling in living mice reveals prominent tissue-specific responses to injury. *J. Immunol.*, **175**, 547–554.
18. Chu, G.C., Dunn, N.R., Anderson, D.C., Oxburgh, L. and Robertson, E.J. (2004) Differential requirements for Smad4 in TGFbeta-dependent patterning of the early mouse embryo. *Development*, **131**, 3501–3512.
19. Wu, R.Y., Zhang, Y., Feng, X.H. and Derynck, R. (1997) Heteromeric and homomeric interactions correlate with signaling activity and functional cooperativity of Smad3 and Smad4/DPC4. *Mol. Cell. Biol.*, **17**, 2521–2528.
20. Heydemann, A., Huber, J.M., Demonbreun, A., Hadhazy, M. and McNally, E.M. (2005) Genetic background influences muscular dystrophy. *Neuromuscu. Disord.*, **15**, 601–609.
21. Matsuda, R., Nishikawa, A. and Tanaka, H. (1995) Visualization of dystrophic muscle fibers in mdx mouse by vital staining with Evans blue: evidence of apoptosis in dystrophin-deficient muscle. *J. Biochem.*, **118**, 959–964.
22. Millay, D.P., Goonasekera, S.A., Sargent, M.A., Maillet, M., Aronow, B.J. and Molkentin, J.D. (2009) Calcium influx is sufficient to induce muscular dystrophy through a TRPC-dependent mechanism. *Proc. Natl. Acad. Sci. USA*, **106**, 19023–19028.
23. Goonasekera, S.A., Lam, C.K., Millay, D.P., Sargent, M.A., Hajjar, R.J., Kranias, E.G. and Molkentin, J.D. (2011) Mitigation of muscular dystrophy in mice by SERCA overexpression in skeletal muscle. *J. Clin. Invest.*, **121**, 1044–1052.
24. Meyers, M.B., Pickel, V.M., Sheu, S.S., Sharma, V.K., Scotto, K.W. and Fishman, G.I. (1995) Association of sorcin with the cardiac ryanodine receptor. *J. Biol. Chem.*, **270**, 26411–26418.
25. Lokuta, A.J., Meyers, M.B., Sander, P.R., Fishman, G.I. and Valdivia, H.H. (1997) Modulation of cardiac ryanodine receptors by sorcin. *J. Biol. Chem.*, **272**, 25333–25338.
26. Zamparelli, C., Macquaide, N., Colotti, G., Verzili, D., Seidler, T., Smith, G.L. and Chiancone, E. (2010) Activation of the cardiac Na(+)-Ca(2+) exchanger by sorcin via the interaction of the respective Ca(2+)-binding domains. *J. Mol. Cell. Cardiol.*, **49**, 132–141.
27. Goldstein, J.A., Kelly, S.M., LoPresti, P.P., Heydemann, A., Earley, J.U., Ferguson, E.L., Wolf, M.J. and McNally, E.M. (2011) SMAD signaling drives heart and muscle dysfunction in a Drosophila model of muscular dystrophy. *Hum. Mol. Genet.*, **20**, 894–904.
28. Bellinger, A.M., Reiken, S., Carlson, C., Mongillo, M., Liu, X., Rothman, L., Matecki, S., Lacampagne, A. and Marks, A.R. (2009) Hypernitrosylated ryanodine receptor calcium release channels are leaky in dystrophic muscle. *Nat. Med.*, **15**, 325–330.
29. Ali, R., Huang, Y., Maher, S.E., Kim, R.W., Giordano, F.J., Tellides, G. and Geirsson, A. (2012) miR-1 mediated suppression of Sorcin regulates myocardial contractility through modulation of Ca(2+) signaling. *J. Mol. Cell. Cardiol.*, **52**, 1027–1037.
30. Meyers, M.B., Fischer, A., Sun, Y.J., Lopes, C.M., Rohacs, T., Nakamura, T.Y., Zhou, Y.Y., Lee, P.C., Altschuld, R.A., McCune, S.A. *et al.* (2003) Sorcin regulates excitation-contraction coupling in the heart. *J. Biol. Chem.*, **278**, 28865–28871.
31. Koitabashi, N., Danner, T., Zaiman, A.L., Pinto, Y.M., Rowell, J., Mankowski, J., Zhang, D., Nakamura, T., Takimoto, E. and Kass, D.A. (2011) Pivotal role of cardiomyocyte TGF-beta signaling in the murine pathological response to sustained pressure overload. *J. Clin. Invest.*, **121**, 2301–2312.
32. Tallquist, M.D. and Soriano, P. (2000) Epiblast-restricted Cre expression in MORE mice: a tool to distinguish embryonic versus extra-embryonic gene function. *Genesis*, **26**, 113–115.
33. Rueda, A., Song, M., Toro, L., Stefani, E. and Valdivia, H.H. (2006) Sorcin modulation of Ca2+ sparks in rat vascular smooth muscle cells. *J. Physiol.*, **576**, 887–901.
34. Barton, E.R., Lynch, G. and Khurana, T.S. (2008) Measuring isometric force of isolated mouse muscles in vitro. In Willmann, R. (ed), *Experimental Protocols for DMD Animal Models*. Treat-NMD Neuromuscular Network, Vol. DMD_M.1.2.002, p. 14.
35. Arimura, T., Helbling-Leclerc, A., Massart, C., Varnous, S., Niel, F., Lacene, E., Fromes, Y., Toussaint, M., Mura, A.M., Keller, D.I. *et al.* (2005) Mouse model carrying H222P-Lmna mutation develops muscular dystrophy and dilated cardiomyopathy similar to human striated muscle laminopathies. *Hum. Mol. Genet.*, **14**, 155–169.